

Determination of Parameters of Linear Quadratic Regulator using Global Best Inertia Weight Modified Particle Swarm Optimization Algorithm

Agbroko Oghenenyoreme Emakpo*, Ogunti Erastus Olarewaju

Department of Electrical and Electronics Engineering, Federal University of Technology, Akure, Ondo State, Nigeria

Received: January 31, 2023, Revised: March 13, 2023, Accepted: March 15, 2023, Available Online: March 20, 2023

ABSTRACT

The characteristics of a linear Quadratic Regulator (LQR) are hinged upon two parameters and they are, the state weighting matrix Q and the Control weighting matrix R. In this study Global Best Inertia Weight modified variant of the particle swarm optimization algorithm was used to determine these two important parameters of an LQR which was then used to control a bus suspension system. The evaluation of the open loop and closed loop showed that the closed loop system attained a steady state in a time of 350.36 seconds compared to the open loop system (47,734.3 seconds) when both systems were subjected to pot hole (step) signal.

Keywords: Linear Quadratic Regulator (LQR), Bus Suspension, Road Profile, Global Best Inertia Weight Modified Particle Swarm Optimization (GBbest IWM PSO) Algorithm.



Copyright @ All authors

This work is licensed under a [Creative Commons Attribution-Non Commercial 4.0 International License](https://creativecommons.org/licenses/by-nc/4.0/).

1 Introduction

LQR is a type of linear optimal control that is based on a state space representation model. It is used for multivariate dynamic systems [1]. It generates a control law by utilizing feedback from its output with its derivatives [2]. Its performance or behaviour, is determined by the state weighting matrix Q and the control weighting matrix R [3]. The values of Q and R, are traditionally ascertained by trial-and-error method [3], and using traditional control methods can be so laborious that at times, it can be so difficult to achieve the best parameters [4], [5], [6]. Due to the aforementioned reason, researchers used various evolutionary algorithms such as particle swarm optimization (PSO) algorithm, Bees algorithm, and Ant Colony among others, to determine the weighting parameters Q and R of an LQR [4]. PSO is an Optimization algorithm which is the result of research by Dr. Russell Eberhart and James Kennedy in 1995 [7]. It is a computational method based on the idea of collective conduct and swarming of populations inspired by the social attitude of bird flocking and fish schooling [8]. The merits of PSO are that it is simple and easy to apply and has quick convergence [9]. It, however, has a disadvantage in that, its particles are sometimes trapped in a local minimum instead of the global minimum, at the later part of convergence thus the final value ends up being a local minimum instead of a global minimum. For this reason, researchers have come up with various modified variants of PSO which include: Discrete PSO, Guaranteed Convergence PSO, Regrouping PSO, Neighborhood Guaranteed Convergence PSO, Niche PSO, Neighborhood search PSO, Immunity-Enhanced PSO, Quantum-Behaved PSO, Multi-Objective Optimization PSO, Hybrid PSO among others. These are meant to raise the diversity of particles and enhance convergence performance [10].

This research used the Global best inertia weight modified variant of PSO (Gbest IWM PSO) to determine the parameters of LQR to control a Bus suspension system.

2 Concept and Review of Related works

The aim of designing and controlling a system with LQR is to return the system to an equilibrium whenever it is displaced from equilibrium in such a way as to minimize a performance index [11]. A performance index is referred to as the addition of deviations of key measurements from their desired state or values. To find the optimal gain, the performance index is first defined and then the solution of the resulting Algebraic Riccati Equation (ARE) is obtained [12]. In this research, we sort to use LQR to control a bus suspension system so that whenever the suspension system is subjected to a road disturbance, it dampens out oscillations as quickly as possible. A suspension system is a device that isolates the body of an automobile from its wheels [13]. It is made up of linkages, damper, and springs that connect a bus to its wheels as shown in Fig. 1.

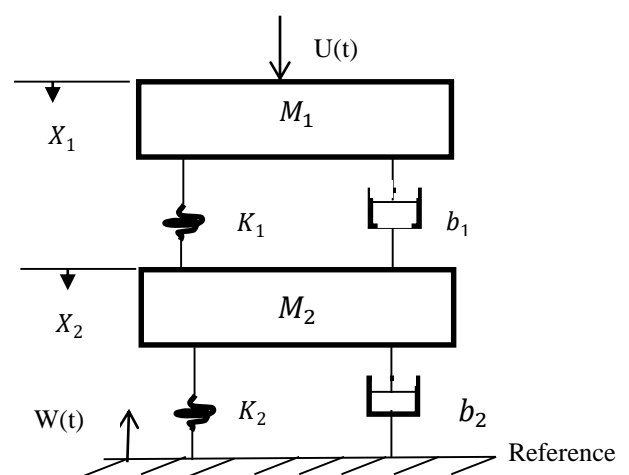


Fig. 1 Diagram of a vehicle suspension system

It is used to decrease the vertical acceleration transmitted to occupants (fare payers and driver) of an automobile. The suspense is designed to provide road handling capacity, load carrying capacity, and passenger comfort.

*Corresponding Author Email Address: everestagbroko@gmail.com

Three types of automobile suspense exist and are active, semi active, and passive. The passive system consists of passive elements such as springs and a damper (shock absorber) [13], [14], [15], [16]. It stores energy by means of springs and dissipates them through the damper. The active system stores, dissipates, and introduces energy into the system. While the active system can be seen as a closed loop system, the passive is an open loop system. The semi active system is a compromise of both the active and passive systems. It doesn't introduce power into the system and hence cannot make the system to be unstable, unlike active suspense.

The bus suspension block diagram shown in Fig. 1 comprises of mass M_1 , which is a quarter of the automobile body mass, also referred to as the sprung mass while mass M_2 is the mass of tires and wheels, also referred to as the unsprung mass, K_1 and K_2 are the spring constant of sprung and unsprung mass respectively, b_1 and b_2 are the damping constant of sprung and unsprung mass respectively, $W(t)$ represents the road disturbance, X_1 and X_2 are the system output while $U(t)$ is the actuating signal. See Table 1.

In PSO, every particle is a prospective solution in the search space [7]. Their movement is determined by two key elements: first is the individual particle's best position and second, the global best position, which is the overall best position that has been generated by the entire particle (swarm). The velocity and position of each particle are updated for each iteration, using Eq. (1) and Eq. (2).

$$V_i^{t+1} = V_i^t + C_1 * rand_1 * (P_{ibest} - X_i^t) + C_2 * rand_2 * (G_{best} - X_i^t) \quad (1)$$

$$X_i^{t+1} = X_i^t + V_i^{t+1} \quad (2)$$

Where V_i^{t+1} is the present particle velocity, V_i^t is the previous particle position, X_i^{t+1} is the present particle position, X_i^t is the previous particle position, P_{ibest} is the particle's best position, G_{best} is the Global best position, C_1 and C_2 are personal and social acceleration coefficients respectively, $rand_1$ and $rand_2$ are random variables between one and four.

To improve control on the scope of the search, Shi and Eberhart introduced inertia weight (W) in 1998 [17] and the updated velocity value is shown in Eq. (3).

$$V_i^{t+1} = W * V_i^t + C_1 * rand_1 * (P_{ibest} - X_i^t) + C_2 * rand_2 * (G_{best} - X_i^t) \quad (3)$$

Further, Arumugan & Rao, in 2006, proposed the Gbest IWM PSO algorithm [18] in which, instead of W being a constant, as seen in Eq. (3) and stipulated by Shi and Eberhart, it was made to be dependent on the values of particle best and global best position for each iteration as shown in Eq. (4).

$$W_i = (1.1 - \frac{G_{best}}{P_{ibest}}) \quad (4)$$

3 Methodology

Based on the diagram of a bus suspension model in Fig. 1 and Newton's law of motion two equations can be derived. They are:

$$U(t) = M_1 \ddot{X}_1 + b_1(\dot{X}_1 - \dot{X}_2) + k_1(X_1 - X_2) \quad (5)$$

$$W(t) = M_2 \ddot{X}_2 + b_2 \dot{X}_2 + b_1(\dot{X}_2 - \dot{X}_1) + k_2 X_2 + k_1(X_2 - X_1) \quad (6)$$

Table 1 Bus suspense parameters (source [19])

Symbol	Parameter	Value/unit
M_1	A quarter of the bus body mass	2,500 kg
M_2	Unsprung mass (tire and wheel)	320 kg
k_1	Spring coefficient of the suspension system	80,000 N/m
k_2	Spring coefficient of wheel and tire	500,000 N/m
b_1	Damping coefficient of the suspension system	350 N.s/m
b_2	Damping coefficient of tire and wheel	15,020 N.s/m

$W(t)$ represents the road disturbance and $u(t)$ is the actuating signal. The state space model of the system was then designed from the state space equations. Consider a representation of the linear time invariant (LTI) system shown in Fig. 2.

$$\dot{x} = Ax + Bu \quad (7)$$

$$y = Cx + Du \quad (8)$$

Where A is n x n state matrix, B is n x r input matrix, C is m x n output matrix, D is m x r direct transmission matrix, x is n x 1 state vector, y is m x 1 output vector and u is r x 1 input vector.

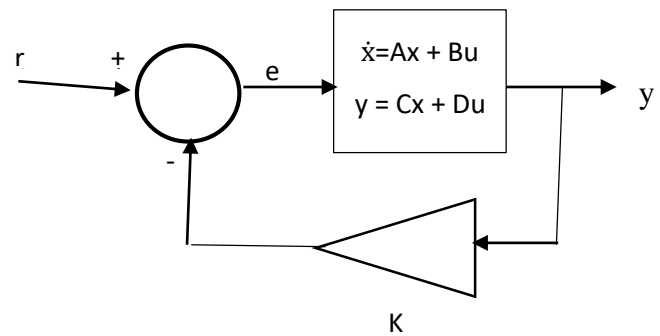


Fig. 2 Block diagram of LTI system.

The cost function of a linear Quadratic regulator is:

$$J = \frac{1}{2} \int_{t_0}^{t_f} (x^T Q x + u^T R u) dt \quad (9)$$

Where Q is a positive semi-definite nxn matrix called the State weighting matrix and R is a positive definite matrix that is called the control weighting matrix. The aim of an LQR design is to achieve an optimal control input u^* that will minimize the cost (objective) function as t_f tends to infinity.

$$u^* = -Kx(t) \quad (10)$$

$$K = R^{-1} B^T P \quad (11)$$

Where K is the optimal control feedback matrix and P is the solution of the ARE which is

$$PA + A^T P + Q - PBR^{-1}B^T P = 0 \quad (12)$$

The performance Index used for this research is Integral Time Absolute Error ie

$$ITAE = \int e/dt \quad (13)$$

Where e from Fig. 2, is the error signal, given as:

$$e = r - ky \tag{14}$$

r is the reference input and y is the system output.

The plant was designed in MATLAB SIMULINK using MATLAB 2020b version, while the Gbest IWM PSO algorithm was coded on the EDITOR window by applying the chosen performance index (ITAE) as its objective function with its parameters indicated in Table 2. The PSO variant was set to run for fifty iterations and the Global best position was recorded. With the aid of the MATLAB “To Workspace” block and MATLAB “sim” command, the Simulink model and the EDITOR were able to interact and results were recorded. Utilizing Eqs. (11) and (12), the values of P, Q, and R were derived.

Table 2 Gbest IWM PSO parameters

S/N	Item	Value	Unit
1	C_1	2	Constant
2	C_2	2	Constant
3	n	4	Number
4	vsize	[1 n]	1xn matrix
5	pop	100	Number
6	minvar	-10000	Meter
7	maxvar	100000	Meter
8	Maximum velocity	22000	m/s
9	Minimum velocity	-22000	m/s

Where n is the number of decision variables, vsize is the matrix size of decision variables, pop is the particle population, minvar is the lower bound of the particles, and maxvar is the upper bound of the particles.

The designed LQR controlled system was then subjected to test signals and the outputs were recorded.

Test signals: Two different types of test signals representing two road conditions were utilized for this study. They can be referred to as road profiles, road disturbances, or road conditions. They are:

Step input- this was modeled to emulate a pot-hole condition of roads. It can be better understood when seen as a vehicle coming out of a pot hole. Fig. 3.

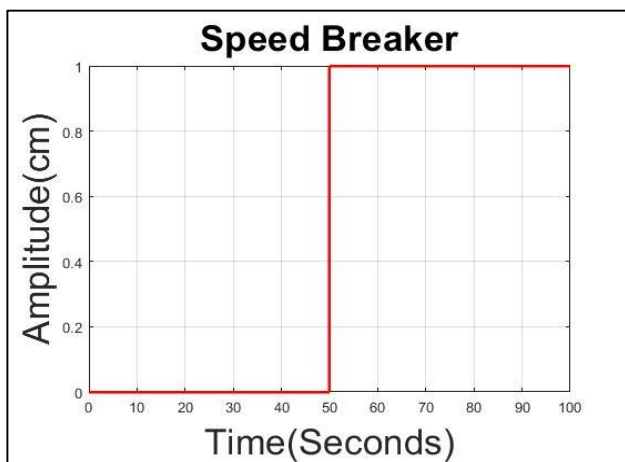


Fig. 3 Step signal

Road Bump or Speed breaker- this is a combination of step input, product block, and sine wave (Fig. 4) to produce the signal shown in Fig. 5 [14].

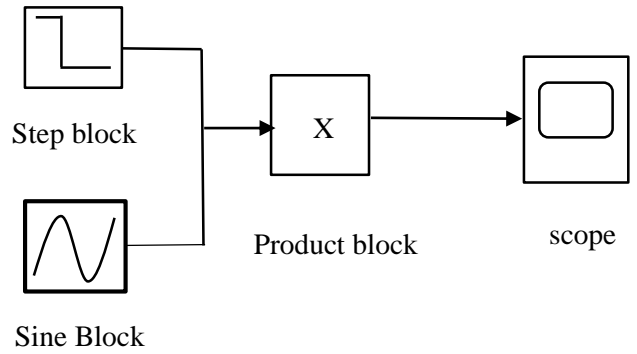


Fig. 4 Design layout of speed breaker

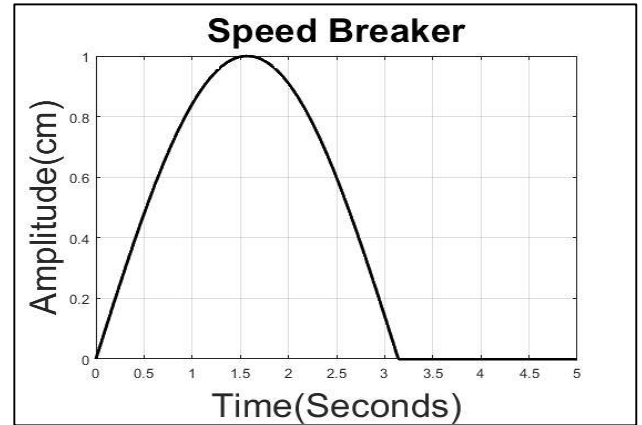


Fig. 5 Speed breaker signal

4 Results and Discussion

The following are the simulation results:

$$G_{best} = [73326\ 74138\ 5757\ 83650], \quad R = \frac{1}{17.9413} \times 10^{-8}$$

$$p = \begin{bmatrix} 6.51 & 0.1567 & -26.1942 & 0.0201 \\ 0.1567 & 106.5042 & -1.363 & -12.5524 \\ -26.1942 & 1.1363 & 187.4036 & 0.0202 \\ 0.0201 & -12.5524 & -0.0202 & 103.1717 \end{bmatrix},$$

$$Q = \begin{bmatrix} 0 & 0 & 0 & 0 \\ 0 & 3 & 0 & 0 \\ 0 & 0 & 0 & 0 \\ 0 & 0 & 0 & 10 \end{bmatrix}$$

The open loop system response is shown in Fig. 6, while Fig. 7 shows the step response of the LQR controlled closed loop. Fig. 8 and Fig. 9 give the system's response to bump input. Fig. 10 and Fig. 11 show the pole locations of the open and closed loop systems in graphical form.

The system response consists of deflection and velocity due to the sprung and unsprung mass. For the deflection of sprung mass, the open loop system attained a maximum peak to trough value of 0.0000289cm to 1.9632×10^{-7} cm at a time of 19.51 seconds and 37.05 seconds respectively, a rise time of 9.95secs and a settling time of 47,734.3secs with a steady state value of 0.00001443 cm. For the velocity of sprung mass, the open loop system has a maximum peak to trough value of 2.4028×10^{-6} to -2.39399×10^{-6} cm/s with a peak time of 9.477 seconds and trough time of 28.726 secs and settling time of 35,000 secs. As regards the deflection of unsprung mass, the maximum peak value was 4.04471×10^{-6} cm/s, maximum trough value was

3.51567×10^{-8} cm/s with a peak time of 18.74 secs, trough time of 39.478 secs, and settling time of 33,357.21 secs. For the velocity of unsprung mass, the maximum peak to trough was 3.63609×10^{-7} cm/s to -3.54501×10^{-7} cm/s, peak and trough times of 8.34 and 29.004 secs respectively, and a settling time of 20,000 seconds (See Fig. 6).

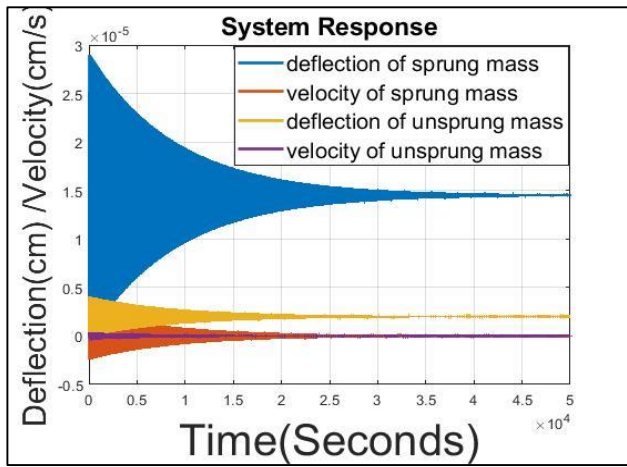


Fig. 6 Open loop system step response.

For closed loop response to pothole signal, as shown in Fig. 7, as regards deflection of sprung mass, the maximum peak to trough value was 1.74477 to 0.444732 cm, the peak time of 19.02 secs, trough time of 37.35 secs, the rise time of 9.94 secs, settling time of 350.36 secs with a steady state value of 1cm. For the velocity of sprung mass, the maximum peak to trough was 0.143799 cm/s to -0.107065 cm/s, peak and trough times of 9.52 and 28.72 secs respectively, settling time of 341.33 secs with a steady state value of 0. As regards the deflection of unsprung mass, the maximum peak to trough was 0.243473 to 0.0601832 cm with a peak time of 18.75 secs, trough time of 37.98 secs, and settling time of 351.3 secs. While for the velocity of unsprung mass, the maximum peak was 0.0224102 cm/s at a time of 8.24 secs, the maximum trough of -0.0162871 cm/s at a time of 28.97 secs and a settling time of 351.3 secs.

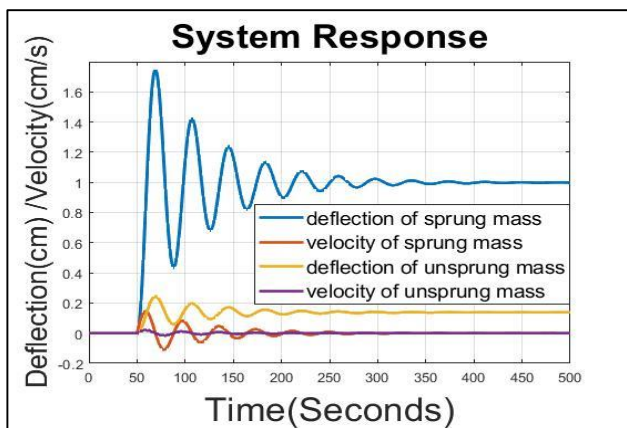


Fig. 7 LQR controlled system step response.

As shown in Fig. 8, with regards to the system open loop response, the deflection of sprung mass attained a maximum peak of 4.7708×10^{-6} cm, maximum trough value of -4.74961×10^{-6} cm, the peak time of 11.04 secs, trough time of 29.56 secs, and settling time of 42,281.1 secs. For the velocity of sprung mass, the maximum peak was $7.66769 \times$

10^{-7} cm/s, the maximum trough of -7.89802×10^{-7} cm/s, the peak time of 3.057 secs, trough time of 20.517 secs, and settling time of 40,000 secs. Furthermore, for the deflection of unsprung mass, the maximum peak to trough was 6.98899×10^{-7} to -6.87874×10^{-7} cm/s at a peak time of 10.001 secs, trough time of 30.301 secs, and settled at 35,000 secs. For the velocity of unsprung mass, the maximum peak was 1.70288×10^{-7} cm/s, maximum trough value was -1.5608×10^{-7} cm/s, the peak time of 3.8544 secs, trough time of 20.214 secs, and settling time of 32,500 secs.

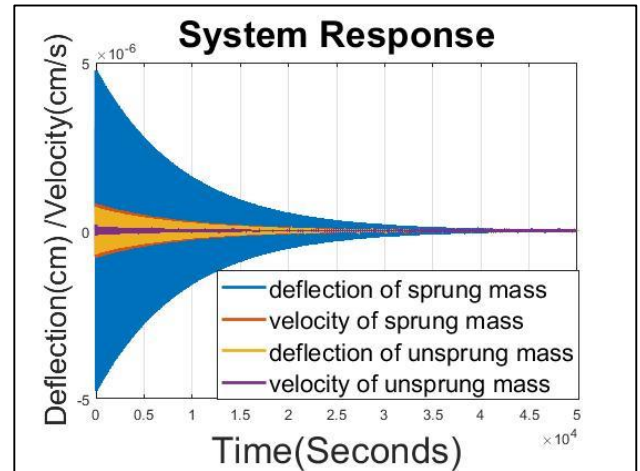


Fig. 8 Open loop bump response.

As shown in Fig. 9, which is the closed loop response to the speed breaker, as regards deflection of sprung mass, the maximum peak was 4.15357×10^{-6} cm, maximum trough of -3.11115×10^{-6} cm, peak time of 10.12 secs, trough time of 29.54secs and settling time of 347.73secs. With reference to the velocity of sprung mass, the maximum peak was 7.33138×10^{-7} cm/s, maximum trough of -6.0146×10^{-7} cm/s, the peak time of 3.01 secs, trough time of 19.25 secs, and settling time of 313.67 secs. For the deflection of unsprung mass, the maximum peak was 6.20629×10^{-7} cm at a time of 10.11 secs, the maximum trough value was -4.57009×10^{-7} cm at a time of 30.29 secs and a settling time of 306.42 secs. Finally, as regard the velocity of unsprung mass, the maximum peak was 1.63343×10^{-7} cm/s, the maximum trough was -1.28999×10^{-7} cm/s, the peak time of 3.82 secs trough time of 20.22 secs, and settling time of 291.303 secs.

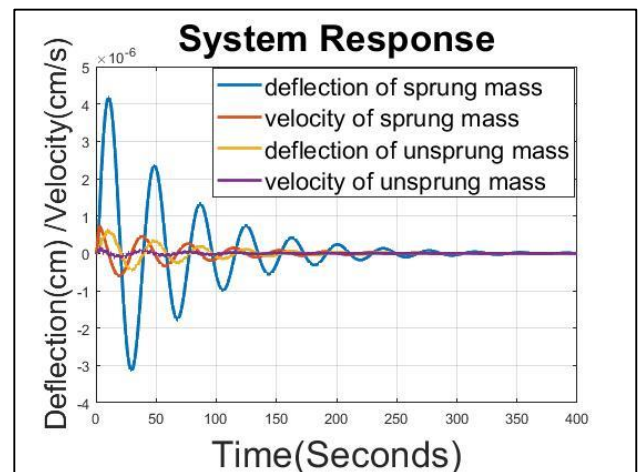


Fig. 9 LQR controlled system bump response.

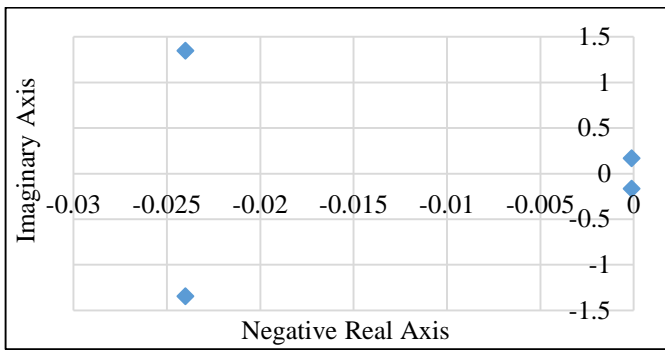


Fig. 10 Open loop system pole location.

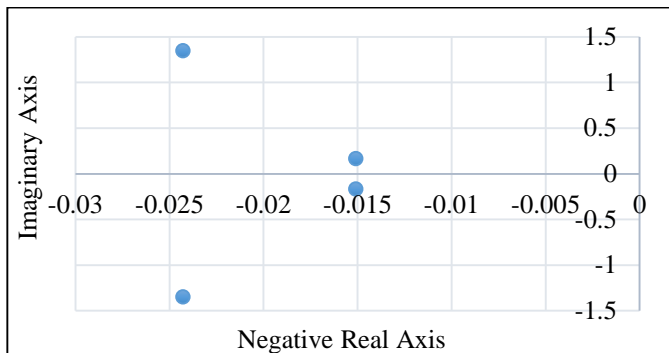


Fig. 11 LQR controlled system pole Location.

From Fig. 10 the open loop pole locations are $-0.024 \pm j1.3477$ and $-0.0001 \pm j0.1659$ while that of the closed loop are at $-0.024 \pm j1.3478$ and $-0.0151 \pm j0.1652$ (Fig. 11). As can be observed, there was a significant relocation of the dominant poles further away from the origin of the s-plane which resulted in a reduction of the system oscillation. Hence the closed loop system damps out oscillation in a shorter duration (350.36 seconds) compared to the open loop (over 47,734.3 seconds) when the systems are subjected to step response. Also, when the system was subjected to a speed breaker, the open loop attained a steady state at about 42,281.1 seconds while the closed loop system attained it at 347.73 seconds considering the deflection of sprung mass only.

5 Conclusion

This research applies Gbest IWM PSO to determine the parameters of an LQR to control a bus suspension system and not a comparison with any other method. However, comparing the open loop system with the closed loop shows significant improvement in the output in terms of reduction in the number of oscillations and settling time due to a drastic relocation of the dominant system poles ($-0.0001 \pm j0.1659$) farther away from the origin of s-plane (Fig. 10 and Fig. 11). The reduction in the number of oscillation and shorter settling time translates into comfort for the occupants of the automobile.

References

- [1] Nath, V. and Mitra, R., 2014. Robust pole placement using linear quadratic regulator weight selection algorithm. *Indian Institute of Technology, Roorkee*, 3, pp. 329-333.
- [2] Anderson, B. & Moore, J., 1989. *Optimal control: linear quadratic methods*, Sydney: Prentice-Hall.
- [3] Al-Mahturi, A. and Wahid, H., 2017. Optimal tuning of linear quadratic regulator controller using a particle swarm optimization for two-rotor aerodynamical system. *International Journal of Electronics and Communication Engineering*, 11(2), pp. 196-202.
- [4] Önen, Ü., Çakan, A. and İlhan, İ., 2017. Particle Swarm Optimization Based LQR Control of an Inverted Pendulum. *Engineering and Technology Journal*, 2(5), pp. 168-174.
- [5] Sen, M.A. and Kalyoncu, M., 2016. Optimal tuning of a LQR controller for an inverted pendulum using the bees algorithm. *J Autom Control Eng*, 4(5), pp. 384-387.
- [6] Hamidi, J., 2012. Control system design using particle swarm optimization (PSO). *International Journal of Soft Computing and Engineering*, 1(6), pp. 116-119.
- [7] Eberhart, R. and Kennedy, J., 1995, October. A new optimizer using particle swarm theory. In *MHS'95. Proceedings of the sixth international symposium on micro machine and human science* (pp. 39-43). IEEE.
- [8] Abdel-Kader, R.F., 2011. Fuzzy particle swarm optimization with simulated annealing and neighborhood information communication for solving TSP. *International Journal of Advanced Computer Science and Applications*, 2(5), pp. 15-21.
- [9] Ahmed, H. and Glasgow, J., 2012. Swarm intelligence: concepts, models and applications. *School Of Computing, Queens University Technical Report*.
- [10] Kumar, A., Singh, B.K. and Patro, B.D.K., 2016. Particle swarm optimization: a study of variants and their applications. *International Journal of Computer Applications*, 135(5), pp. 24-30.
- [11] Burns, R., 2001. *Advanced control engineering*. Elsevier.
- [12] Alias, N.A., 2013. *Linear quadratic regulator (LQR) controller design for inverted pendulum* (Doctoral dissertation, Universiti Tun Hussein Malaysia).
- [13] Agharkakli, A., Sabet, G.S. and Barouz, A., 2012. Simulation and analysis of passive and active suspension system using quarter car model for different road profile. *International Journal of Engineering Trends and Technology*, 3(5), pp. 636-644.
- [14] Ahmed, A.A., 2021. Quarter car model optimization of active suspension system using fuzzy PID and linear quadratic regulator controllers. *Global Journal of Engineering and Technology Advances*, 6(03), pp. 088-097.
- [15] Al-Mutar, W.H. and Abdalla, T.Y., 2015. Quarter car active suspension system control using fuzzy controller tuned by pso. *International journal of computer applications*, 127(2), pp. 38-43.
- [16] Ghazaly, N.M., Ahmed, A.E.N.S., Ali, A.S. and Abd El-Jaber, G.T., 2016. H_{∞} Control of Active Suspension System for a Quarter Car Model. *International Journal of Vehicle Structures & Systems (IJVSS)*, 8(1), pp. 35-40.
- [17] Shi, Y. and Eberhart, R., 1998, May. A modified particle swarm optimizer. In *1998 IEEE international conference on evolutionary computation proceedings. IEEE world congress on computational intelligence (Cat. No. 98TH8360)* (pp. 69-73). IEEE.
- [18] Arumugam, M.S. and Rao, M.V.C., 2006. On the performance of the particle swarm optimization algorithm with various inertia weight variants for computing optimal control of a class of hybrid systems. *Discrete Dynamics in Nature and Society*, 2006, pp. 1-17.
- [19] Nurhadi, H., 2010. Study on Control of Bus Suspension System. Seminar Nasional Tahunan Teknik Mesin, *Department of Mechanical Engineering, Institut Teknologi Sepuluh Nopember (ITS)*, pp. 229-234.